Saudi Pharmaceutical Journal 29 (2021) 467–477

Contents lists available at ScienceDirect

Saudi Pharmaceutical Journal

journal homepage: www.sciencedirect.com

Original article

Formulation and *in vitro* evaluation of topical nanosponge-based gel containing butenafine for the treatment of fungal skin infection

Mohammed Muqtader Ahmed [a,*], Farhat Fatima [a], Md. Khalid Anwer [a,*], Elmutasim Osman Ibnouf [b], Mohd Abul Kalam [c], Aws Alshamsan [c], Mohammed F. Aldawsari [a], Ahmed Alalaiwe [a], Mohammad Javed Ansari [a]

[a] Department of Pharmaceutics, College of Pharmacy, Prince Sattam Bin Abdulaziz University, P.O. Box 173, AlKharj 11942, Saudi Arabia
[b] Department of Pharmaceutical Microbiology College of Pharmacy, Prince Sattam Bin Abdulaziz University, P.O. Box 173, AlKharj 11942, Saudi Arabia
[c] Nanobiotechnology Unit, Department of Pharmaceutics, College of Pharmacy, King Saud University, P.O. Box 2457, Riyadh 11451, Saudi Arabia

ARTICLE INFO

Article history:
Received 18 January 2021
Accepted 13 April 2021
Available online 27 April 2021

Keywords:
Nanosponges
Topical gel
In-vitro diffusion
Antifungal study
Flux

ABSTRACT

In the current study, four formulae (BNS1-BNS4) of butenafine (BTF) loaded nanosponges (NS) were fabricated by solvent emulsification technology, using different concentration of ethyl cellulose (EC) and polyvinyl alcohol (PVA) as a rate retarding polymer and surfactant, respectively. Prepared NS were characterized for particle size (PS), polydispersity index (PDI), zeta potential (ZP), entrapment efficiency (EE) and drug loading (DL). Nanocarrier BNS3 was optimized based on the particle characterizations and drug encapsulation. It was further evaluated for physicochemical characterizations; FTIR, DSC, XRD and SEM. Selected NS BNS3 composed of BTF (100 mg), EC (200 mg) and 0.3% of PVA showed, PS (543 ± 0.67 nm), PDI (0.330 ± 0.02), ZP (−33.8 ± 0.89 mV), %EE (71.3 ± 0.34%) and %DL (22.8 ± 0.67%), respectively. Fabricated NS also revealed; polymer-drug compatibility, drug-encapsulation, non-crystalline state of the drug in the spherical NS as per the physicochemical evaluations. Optimized NS (BNS3) with equivalent amount of (1%, w/w or w/v) BTF was incorporated into the (1%, w/w or w/v) carbopol gel. BTF loaded NS based gel was then evaluated for viscosity, spreadability, flux, drug diffusion, antifungal, stability and skin irritation studies. BNS3 based topical gels exhibited a flux rate of 0.18 (mg/cm^2.h), drug diffusion of 89.90 ± 0.87% in 24 h with Higuchi model following anomalous non-Fickian drug release. The BNS3 based-gel could be effective against pathogenic fungal strains.

1. Introduction

Nanomedicine brings about the revolutionary improvement and development in the medical sciences, applying nanotechnology in the medicines by employing nanoscale materials could be useful to monitor, control, construct and repair the biological systems (Ventola et al., 2010). In recent years, pharmaceutical scientists have explored nanotechnology for temporal and targeted drug delivery systems (Radaic et al., 2020). There have been various nanocarriers systems including metallic, polymeric-nanoparticles (Anwer et al., 2016), nano-suspension, nano-tubes (Bianco et al., 2005), nanofibers (Sousa et al., 2020) and nanosponges (NS) (Ahmed et al., 2020a) extensively used for the effective treatment of infectious diseases, besides the commercial application in the consumer products. Reports have shown that apremilast loaded nanoparticles increased drug solubility, bioavailability and efficacy in the treatment of psoriasis (Anwer et al., 2019). Smart hand-wash prepared by *Azadirachta indica,* silver nanoparticles was found effective against the pathogenic microbes contrary to commercial hand sanitizers (Nomura and Terwilliger, 2019). Nanoparticle matrix of chitosan showed potential antifungal activity against fungal pathogens (Bautista-Baños et al., 2017). Nanoemulsion of olive oil showed a marked enhancement in permeability and efficacy of amphotericin B (Hussain et al., 2016). Nanosponges (NS) prepared by β-cyclodextrin proclaimed to enhance the solubility of BCS class

* Corresponding authors at: Department of Pharmaceutics, College of Pharmacy, Prince Sattam Bin Abdulaziz University, Al-Kharj, Saudi Arabia.
E-mail addresses: muqtadernano@gmail.com (M.M. Ahmed), mkanwer2002@yahoo.co.in (M.K. Anwer).
Peer review under responsibility of King Saud University.

Production and hosting by Elsevier

https://doi.org/10.1016/j.jsps.2021.04.010
1319-0164/

II and IV drugs (Kang et al., 2019). Nanosponges (NS) have been tested to deliver drugs, biocatalysts and gases, adsorption of toxic materials (Varan et al., 2020). Recently an increase in interest towards the development of nanosponges based drug delivery system was observed in order to improve the solubility and bioavailability of poorly soluble drugs (Kang et al., 2019; Omar et al., 2020). NS are proved to be an innovative spherical nanocarrier with wide cavities and large porous surface into which both lipophilic and hydrophilic drug entities can be encapsulated (Conte et al., 2014; Appleton et al., 2020; Shoaib et al., 2018; Rao et al., 2018; Trotta et al., 2012), and overcome the drug limitations (Manchanda and Sahoo, 2017; Rao et al., 2018; Trotta et al., 2012). Fabricated nano matrix could be bestowed in oral, parenteral and topical dosage forms (Manchanda and Sahoo, 2017).

Nanocarriers in topical delivery systems are more manifested due to their increased penetrability and passive accumulation at the target site (Vyas et al., 2014). Topical drug delivery systems (TDDS) can be manufactured easily into liquid, solid and semisolid dosage forms, chiefly intended to deliver a therapeutically effective concentration of drug in the skin or mucosal layers (Luís et al., 2016).

Topical formulations possess certain merits over the peroral or parenteral dosage forms including, low risk of unavoidable adverse reaction due to systemic drug distribution and patient compliance. Dermatologists preferred the topical semisolid formulations for the treatment of superficial skin infections and disease conditions (Chang et al., 2013).

The skin covers and protects the body against the environmental threats and it's one of the largest organ, representing approximately 2 m^2 of a total body area. Skin considered to be an impermeable membrane that acts as a barrier for the external stimuli and xenobiotic. Therefore, it's a challenge for the formulation scientists to develop successful topical dermal dosage forms, especially to treat dermal infections and disease states (Bergfelt, 2009). The prevalence of superficial fungal infections (SFI) of skin, hair, and nails has been increased worldwide. The progression of fungal infections can be rapid and serious due to compromising immune function (Bongomin et al., 2017). Many epidemiological studies are reflecting the predominance of SFI in the Arabian Peninsula. There are about 20–25% of population affected by fungal infections globally. The fungal infection includes; dermatophytes and candidiasis triggered mainly in a tropical regions and humid environment with an ambient temperature (25–28 °C) that favors the fungal germination (Yapar, 2014). Besides these implications, the current trends of migration, urbanization, poor sanitization, sports activity and occlusiveness of the skin by clothing also supports the SFI. The cyclic encounter of fungal infection renders poor performance, introverted of the workforce with financial encumbrance on the national health budget.

Antifungal drugs incorporated in nanocarriers showed excellent results compared with conventional drug carriers (Garg et al., 2020). The SFI persists on the skin, genital region, nails and hairs. Fungal infection therapy considered to be refractory due to the lack of clinical evidence and deprived physicochemical properties of azole (miconazole, fluconazole) and allylamines (terbinafine, butenafine) derivatives (Gintjee et al., 2020).

Butenafine HCL (BTF), the derivative of benzylamine is a new generation antimycotic compound with potent fungicidal activity. It acts by inhibiting the sterol synthesis thereby blocking the squalene epoxidation stage in fungi (Arika et al., 1990). Butenafine is sparingly soluble in water but readily soluble in methanol, ethanol, dichloromethane, and chloroform with molecular weight less than 400 Da makes it suitable drug candidates for NS (Fig. 1). Currently, butenafine sustained release topical dosage form is neither available in the market nor any research published in the scientific literature. The objective of the present study was to develop the BTF loaded NS into the carbopol polymeric gel for prolonged drug release and permeation. The developed formulation may enhance the drug permeation deeper into the skin layer, which might eradicate the fungal infections of the dermal region by which cyclic recurrence of infection possibly will be terminated.

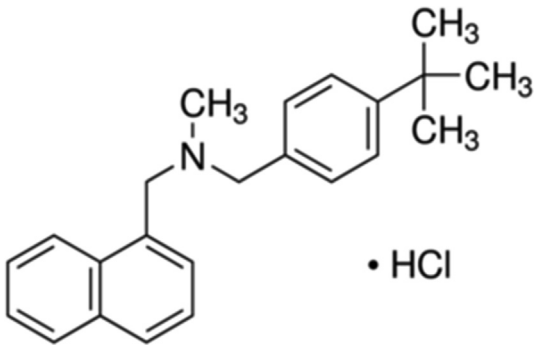

Fig. 1. Chemical structure of Butenafine hydrochloride.

2. Materials and method

2.1. Chemical and solvents

Butenafine Hydrochloride (BTF) was obtained as a gift sample from Jazeera Pharmaceutical Industries (JPI), Riyadh. Ethyl cellulose, Polyvinyl Alcoho (PVA, Mole wt- 85,000–124,000), Dichloromethane and Carbopol 934P were purchased from "Sigma-Aldrich (St. Louis, Missouri, USA)". All other reagents and chemicals utilized were of analytical grades. Deionized water (18.2 MΩ·cm at 25 °C) were collected from Millipore Mill-Q Gradient A-10 water-purification systems (Bedford, MA, United States).

2.2. Analysis

Analysis of BTF and their prepared formulation samples was carried out using RP-HPLC according to reported method (Bhosale and Rajput, 2011). Briefly, RP-HPLC equipped with UV detector using C18 column, mobile phase consisting of methanol and water (90:10, v/v) at flow rate 1 mL/min. Detection was performed at 254 nm. The calibration curve of BTF was plotted using concentration (50, 75, 100, 150 and 200 μg/mL) Vs peak area. The regression coefficient of correlation was measured (R^2) 0.9973.

2.3. Development of BTF loaded NS

BTF loaded NS (BNS) were prepared by the emulsion solvent evaporation technique (ESE-Tech) using the drug (BTF) 100 mg and polyvinyl alcohol (PVA) 0.3%, w/v, compositions of formulations were tabulated in Table1. Briefly, organic phase was prepared by dissolving ethyl cellulose (EC) (100–250 mg) and BTF in 20 mL dichloromethane (DCM). Separately, an aqueous phase was prepared composed of (0.3%, w/v) PVA in 100 mL of deionized water. Thereafter, the organic phase was emulsified dropwise into the aqueous phase by ultrasonication, at power 65% W for 3 min (10 s on-off cycles) (Ahmed et al., 2020a). The formed NS was stabilized by PVA, which avoid particle agglomerations. Thereafter, the dispersion was kept on thermostatically controlled magnetic stirrer "(Fisher Isotemp Hot Plate and Stirrer, Canada)" with continuous stirring at 1000 rpm under atmospheric pressure and temperature for 24 h (Pawar et al., 2019). After complete evaporation of the organic solvent, the BNS were washed three times with ultra-purified water to remove the adsorbed PVA, NSs were then collected by ultracentrifugation at 16,900g and 4 °C for 30 min "

Table 1
Preparation and characterization Butenafine loaded Nanosponges.

Formulation code	Nanosponge composition			Particle characterization and drug analysis				
	BTF (mg)	EC (mg)	PVA (%w/v)	PS (nm)	PDI	ZP (mV)	EE (%)	DL (%)
BNS1	100	100	0.3	310 ± 0.16	0.421 ± 0.06	−18.4 ± 0.34	51.2 ± 0.67	8.4 ± 0.42
BNS2	100	150	0.3	410 ± 0.98	0.490 ± 0.04	−28.6 ± 0.87	60.5 ± 0.51	18.6 ± 0.78
BNS3	100	200	0.3	543 ± 0.67	0.330 ± 0.02	−33.8 ± 0.89	71.3 ± 0.34	22.8 ± 0.67
BNS4	100	250	0.3	808 ± 0.32	0.620 ± 0.04	−31.4 ± 0.87	78.4 ± 0.87	20.9 ± 0.0.87

Butenafine (BTB), EC (Ethyl cellulose), PVA (polyvinyl alcohol), PS (Particle size), PDI (Polydispersity index), ZP (zeta-potential), EE (Entrapment efficiency), DL (Drug loading).

(Eppendorf, centrifuge 5418R, Hamburg, Germany)" and freeze-dried "(Millirock Technology, Kingston, NY, USA)".

2.4. Development of topical gel impregnated with optimized NS (BNS3)

Based on the size, *PDI*, ZP, EE and DL evaluation, BNS3 was optimized and selected to incorporate into carbopol gel. The optimized BNS3 (BTF, 1% w/w) was incorporated into using carbopol 934P as gelling agent (1%, w/v) in a 30:70 ratio of propylene glycol and deionized water. Further, methyl paraben (0.1%, w/w) was added as a preservative, transparency was achieved and pH was adjusted by adding triethanolamine (Yang et al., 2016). The developed gel was then continuously stirred on a shaft stirrer at 500 rpm for about 6 h and kept overnight to achieve complete hydration (Moglad et al., 2020).

2.5. Particle characterization

The particle size analysis of BTF loaded NS (BNS1-BNS4) was performed by using "Malvern Zetasizer NanoZS (Malvern Instruments, UK)". The sample under investigation was diluted with distilled water (1: 200) and filled in disposable polystyrene cuvette. Measurement of particle size and *PDI* was done based on the dynamic light scattering (DLS) theory. The same procedure was followed for the measurement of zeta potential (ZP) except using electrode cuvette (Ahmed et al., 2019). All the samples were tested in triplicate (n = 3).

2.6. Measurement of entrapment efficiency (EE) and drug loading (DL)

Percent entrapment efficiency (% EE) and drug loading (% DL) were estimated by collecting the filtrate from the dispersion after ultracentrifugation at 16,900 × g and 4 °C for 30 min "(Eppendorf, centrifuge 5418R, Hamburg, Germany)". The supernatant was collected, filtered and analyzed by RP-HPLC at 254 nm to determine the BTF concentrations (Bhosale and Rajput, 2011). The % EE and % DL of BTF loaded NS were calculated by using following equations (Ahmed et al., 2019).

$$\%EE = \frac{(Initial\ amount\ of\ drug\ added - Drug\ amount\ in\ supernatant)}{Initial\ amount\ of\ drug\ added} \times 100 \quad (1)$$

$$\%DL = \frac{(Initial\ amount\ of\ drug\ added - Drug\ amount\ in\ supernatant)}{Total\ amount\ weight\ of\ nanosponges} \times 100 \quad (2)$$

2.7. Evaluation of optimized NS

Based on particle size, *PDI*, ZP, %EE, and %DL, the BTF loaded NS (BNS3) was found the best formulation. Therefore, BNS3 was chosen and subjected for further evaluation.

2.7.1. Fourier transform infrared (FTIR) spectroscopy

The FTIR spectra of pure BTF, Blank NS and optimized BNS3 NS were recorded and interpreted for the possible chemical interactions. The transparent pellets of these samples were prepared by mixing each of these components with potassium bromide and FTIR spectras were recorded in the region of 4000–400 cm^{-1} "(FTIR Spectrophotometer, Jasco-Japan).

2.7.2. Differential scanning calorimetry (DSC)

Thermal peaks of pure drug BTF, Blank NS and optimized NSs (BNS3) were evaluated for drug encapsulation. The samples (5 mg) were enclosed in aluminum pan and heated at a rate of 10 °C/min in the temperature range of 30–300 °C, the device was purged with inert N_2 gas at flow rate 20 mL/min "(Scinco N650, made in Italy)" during the study.

2.7.3. Scanning electron microscopy (SEM)

SEM images of the optimized BNS3 NS was taken by scanning electron microscope "(JEOL, JSM-SEM 5200, Tokyo, Japan)". A concentrated aqueous suspension of samples was spread over a slide and dried under vacuum. Surface topography was captured by the machine operated at 15 kV acceleration voltage. The sample was shadowed in a cathode evaporator with a gold layer of 20 nm thick. Microphotograph was captured and processed by an image processing program and individual NS diameters was measured and surface characteristic feature of the BNS3 was examined (Anwer et al., 2019).

2.8. Characterization of topical gel impregnated with nanosponge

Based on the physical and physicochemical characteristics BNS3 was selected and incorporated into the polymeric gel. The developed gel was further evaluated.

2.8.1. pH determination

The pH of BTF loaded NS based topical gel was checked directly by dipping the electrode into the gel and allowed to equilibrate, then the pH was measured by calibrated pH meter "(Edge pH series, Hanna instruments)" maintained at 25 °C (Ahmed et al., 2020b). The sample was tested in triplicate.

2.8.2. Viscosity determination

The viscosity of the developed NS based gel was measured using Brookfield viscometer (Prime Rheometer DV 1; Middleboro, USA). Viscosity was measured at 25 °C at 100 rpm (Ahmed et al., 2020b).

2.8.3. Spreadability measurement

The spreadability test was performed by in-house fabricated apparatus. The apparatus consists of wooden block with a pulley at one end. The spreadability was measured by slip and drag of gel. A glass slide was fixed on wooden block and approximately one gram of gel was sandwiched between the two 5 × 20 cm glass plates. The top plate was laden with 100 g for 40 sec. The initial

and final gel spreading diameters were noted and percentage spreadability was calculated by following equation.(Moglad et al., 2020; Shukr and Metwally, 2013).

$$\textbf{Spreadability} = \frac{\mathbf{D2} - \mathbf{D1}}{\mathbf{D1}} \times 100 \quad (3)$$

Where; D1 was initial diameter of gel before weight load, and D2 was final diameter of gel after load.

2.8.4. Drug content estimation

The percentage of drug content was estimated in nanosponge loaded gel. Drug was extracted by dispersing the known quantity of gel in methonolic:HCl (1:1) and sonicated for 30 min, then filtered and analyzed for drug content by RP HPLC at 254 nm (Bhosale and Rajput, 2011).

2.8.5. Determination of partition coefficient, permeation coefficient and flux of drug

Organic solvent (octanol) and aqueous phase (deionized water) were mixed in a 1:1 ratio and kept for saturation for 1 h. Optimized BNS3 gel (equivalent to pure drug BTF 100 μg) was added in separating funnel containing octanol and water solvent mixture, flask was shaken vigorously and then allowed to stand for 24 h at controlled room condition. Both the phases were separated, the solvent then filtered and drug content was determined in both organic and aqueous phases by RP HPLC at 254 nm. The partition coefficient was determined by following equation:

$$\mathrm{Ko/w} = \frac{BTF\ conc.\ in\ octanol}{BTF\ conc.\ in\ water} \quad (4)$$

Further the permeability coefficient (K_p) was calculated by an empirical relationship between $K_{o/w}$ and molecular weight of BTF (MW 353.93 g/mol, BTF). Permeability coefficient (K_p) was measured as per the following equation (Mahajan et al., 2018).

$$Log\ K_p(cm/h) = -2.72 + 0.71\ LogK_{o/w} - - 0.0061\ X\ (MW) \quad (5)$$

Flux of drug was also determined by using the following equation (Moglad et al., 2020).

$$Flux = log\ K_pX\ (aqueous\ solubility\ of\ drug) \quad (6)$$

2.9. Drug diffusion and release kinetics

Drug diffusion study was performed by using Franz diffusion cell mounted with artificial cellophane membrane (MWCO 14 kDa). The sample BNS3, BNS3 loaded topical gel (1 g) and marketed formulation (Derfina®) were placed in the donor compartment, separately. The receptor chamber was filled with phosphate buffer (pH 7.2), kept on thermostatically controlled magnetic stirrer at temperature (37 ± 0.5 °C) and magnetic bar stirring (50 rpm). At pre-determined time intervals 1 mL of drug-diffused solution was withdrawn and replaced with the equivalent volume by fresh release medium, the aliquots were analyzed by RP HPLC at 254 nm. The amount of drug released was calculated and cumulative (%) drug released vs time graphs for BNS were plotted.

2.9.1. Calculation of drug release kinetics from porous NS matrix

Drug release data was fitted in four kinetic models, zero-order, first order, Higuchi and Korsmeyer–Peppas kinetics models and regression analysis was performed.

$$Q_t = Q_0 + k_0 t(zero - order) \quad (7)$$

$$logQ_t = logQ_0 - - k_1 t\ /\ 2.303\ (first - order) \quad (8)$$

$$Q_t = k_H t^{1/2}(Higuchi) \quad (9)$$

$$M_t/\ M_\infty = kt^n(Korsmeyer - Peppas) \quad (10)$$

Where, Q_t (drug dissolved over time t), Q_0 (initial amount of drug dissolved in diffusion medium i.e equal to zero), k_0 (zero order kinetics constant), k1 (first-order rate constant), $k_H t^{1/2}$ (Higuchi model constant). M_t and M_∞ are cumulative drug release at time t and infinite time, respectively; k is rate constant of NS particle's structural and geometric characteristics feature, t is the release time and *n* denotes diffusional exponent indicating release mechanism. When $n = 0.45$ (Case I or Fickian diffusion), $0.45 < n < 0.89$ (anomalous behavior or non-Fickian transport), $n = 0.89$ (Case II transport) and $n > 0.89$ (Super Case II), based on the exponent value release mechanisms were reported (Pudjiastuti et al., 2020).

2.9.2. Comparative release studies of BNS3 gel and marketed butenafine cream

In vitro drug release of BTF nanosponge loaded gel was compared with marketed butenafine topical gel (1%, w/w cream). All the parameters and conditions for diffusion study were mimicked in this study (Moglad et al., 2020).

2.10. In vitro antifungal studies

Antifungal study was done to determine the efficacy of the BNS3 gel against *Candida albicans (C. albicans)* and *Aspergillus niger (A. niger)* fungal strains. Sabouraud dextrose agar (SDA) media,

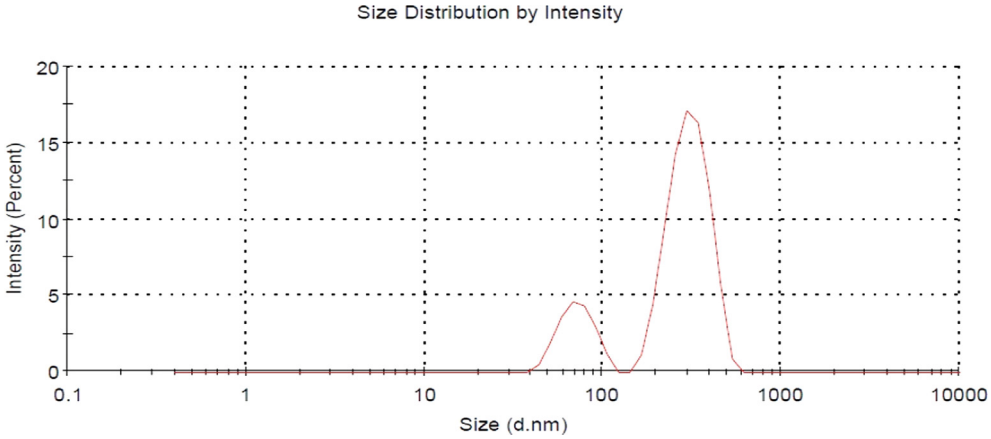

Fig. 2. Particle size distribution of BNS3 nanosponge.

standard paper disc and sterilized Petri dishes were used in this study. SDA (20 mL) treated with the test organism (0.5 mL) was allowed to solidify in the sterilized Petri-plate. Paper discs (Whatman filter No. 42, diameter of 4 mm), soaked in test solutions; BTF, BNS3 Gel and marketed Butenafine gel (1%, w/w cream). Pretreated paper discs were carefully placed on the surface of SDA media under a sterile condition. Then Petri plates were incubated at 27 °C for 48 h (Moglad et al., 2020). The diameters of the zones of inhibition (ZI) were observed and measured using ruler. Readings were taken in triplicate (n = 3) in millimeter unit.

2.11. Stability studies

Developed BNS3 loaded topical gel was assessed for stability test for 90 days by exposing the sample(s) at room temperature (25 ± 2 °C) and accelerated condition (50 ± 2 °C, 75%RH) in

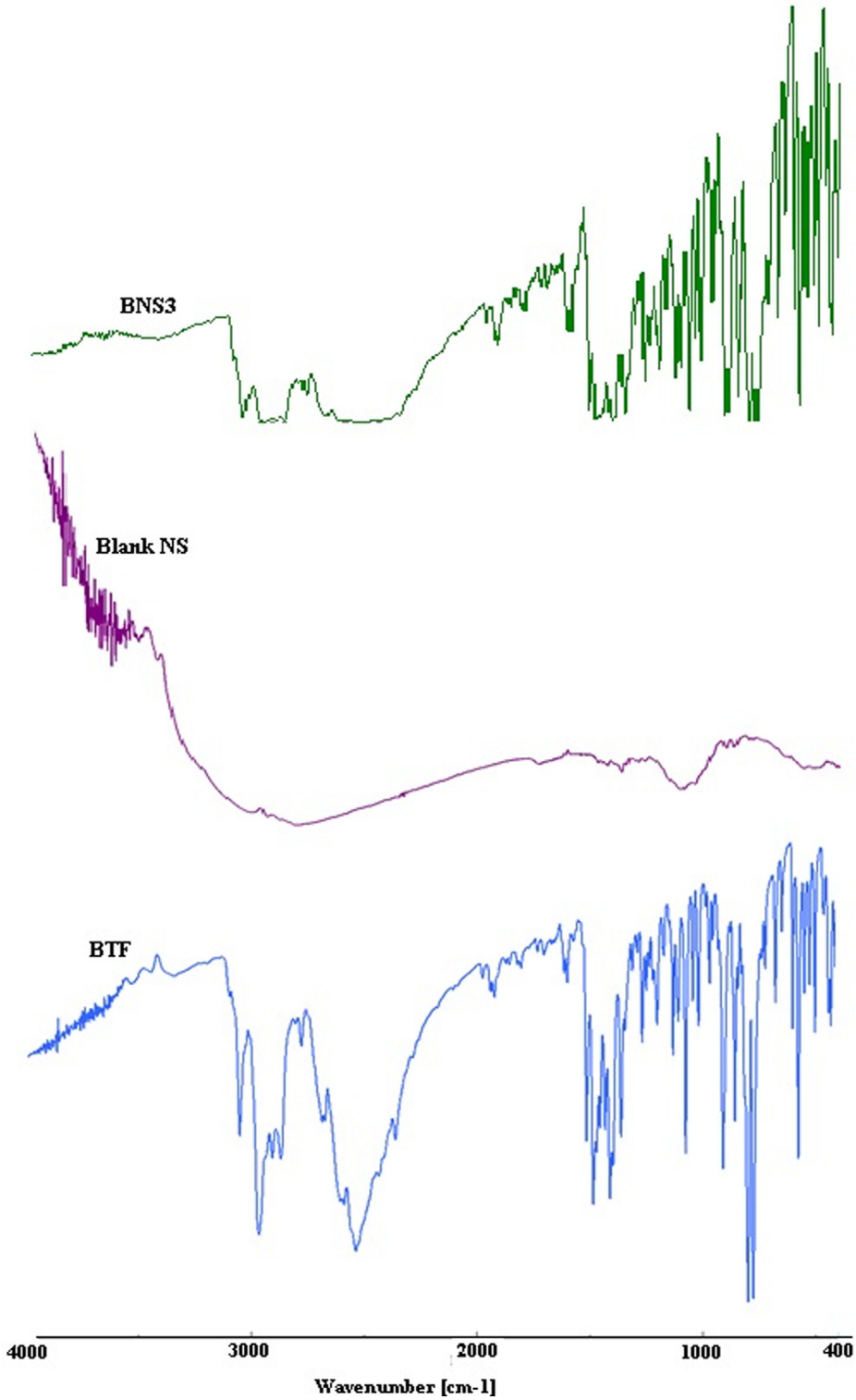

Fig. 3. FTIR Spectrum of drug (BTF), Blank NS and optimized BNS3 nanosponge.

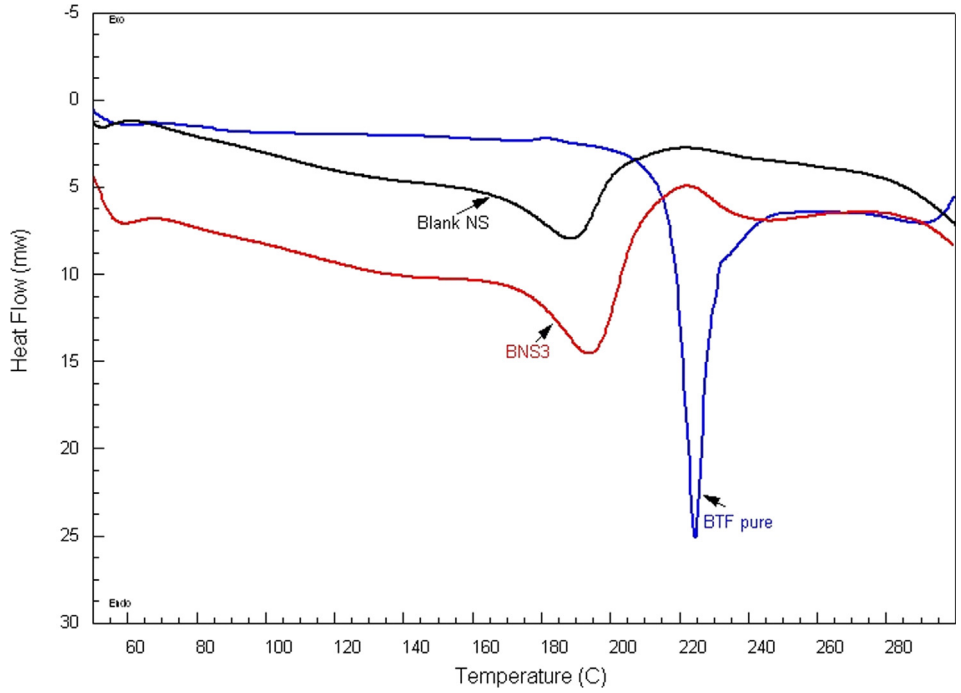

Fig. 4. Thermograms of drug (BTF), Blank NS and optimized BNS3 nanosponge.

programmable environmental test chamber (Parameter Generation and Control). BNS3 gel after a stability period of 12 weeks was tested for particle size and drug release (Ahmed et al., 2020a,b). Thereafter, the release data of both before and after stability test was computed into the similarity index equation as referred in SUPAC guidelines.

$$\boldsymbol{f}2 = 50\mathbf{Xlog}\{[1 + (1/\mathbf{n})\sum_{\boldsymbol{t}-1}^{\boldsymbol{n}}(\boldsymbol{Rt} - \boldsymbol{Tt})2] - 0.5\mathbf{X}100\} \quad (11)$$

where, f_2 means similarity factor, n stands for dissolution time, R_t and T_t denote reference and test dissolution values at time t.

2.12. Statistical analysis

All the data were analyzed by one-way analysis of variance (ANOVA), using "Dennett's test". A difference was considered statistically significant when $\rho \leq 0.05$. All the tests samples were assessed In triplicate and data were expressed as a mean ± standard deviation.

3. Results and discussion

3.1. Particle characterizations

The developed BTF loaded NS (BNS) showed size in the range of (310 ± 0.16 nm to 808 ± 0.32 nm), *PDI* (0.330 ± 0.02 to 0.422 ± 0.04) and, ZP (−33.8 ± 0.89 to −18.4 ± 0.34 mV). Further, the particle size, ZP and *PDI* were found to be increased with an increase in EC polymer concentration (Table 1). The data of the zeta potential and *PDI* exhibits that all the NS were negatively charged with sufficient inter-particle repulsive force (≥33 mV) with the narrow size distribution as the *PDI* value was found to be less than ≤ 0.7, the results interrelated with the statement presented in the review of Danaei et.al (Danaei et al., 2018). Based on the particle characterization, BNS3 could be the optimized NS with the particle size (543 ± 0.67 nm), *PDI* (0.330 ± 0.12) and zeta potential of −33.8 ± 0 .89 mV. Particle size distribution by intensity for optimized BNS3 is represented in Fig. 2.

3.2. Entrapment efficiency and drug loading calculation

Entrapment efficiency of developed NS (BNS1-BNS4) was found to be in the range of (51.2 ± 0.67% to 78.4 ± 0.87%), the results are given in Table 1. Amount of the drug entrapped was found to be

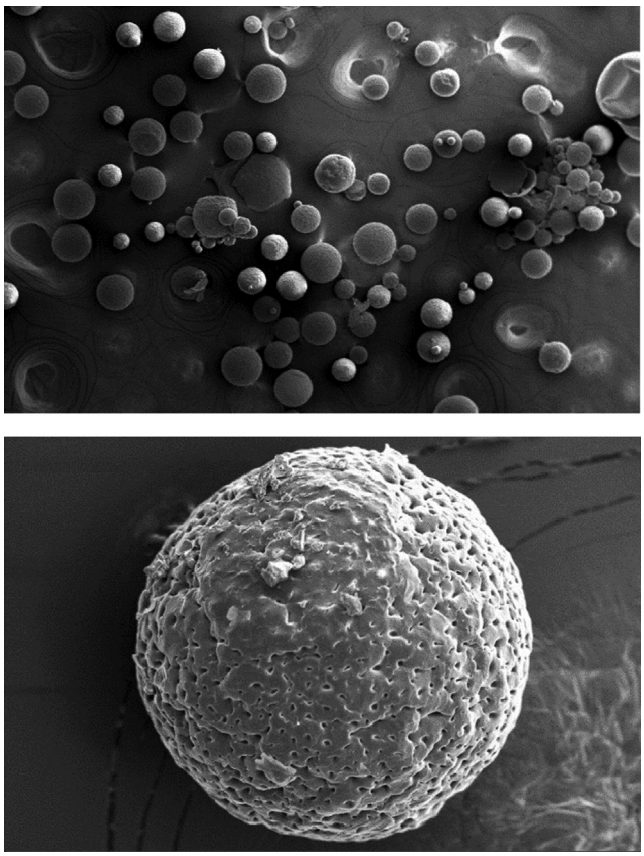

Fig. 5. SEM picture - surface morphology of BNS3 nanosponges.

increased with the higher particle size and EC polymer concentration. In contrast, less particle size would be responsible for low entrapment efficiency, as the small particles could have more surface area to give more prospect for drug escape from the porous nanocage (Srikar and Rani, 2019). BTF being water insoluble drug that enforce its maximum entrapment in nanocarriers. BTF represents higher drug-polymer interaction and miscibility in organic solvent (DCM). Therefore, higher concentration of EC polymer leading to maximum drug entrapment in NS. This result was in agreement with Sharma et.al (Sharma and Pathak, 2011). BTF loading in NSs was found to be in the range of (8.4 ± 0.42% to 22.8 ± 0.67%). BNS3 showed the maximum drug loading. The loading of drug was found to be increase by increasing the EC concentration. However further increment in the EC polymer concentration in case of BNS4 decreases the drug loading, which could be due to the maximum loading of drug in the polymer reached the % DL capacity. Furthermore, an increase in the amount of EC polymer, increased the viscosity of the organic phase leading to a decrease in the drug diffusion from organic phase to an aqueous phase leading to the formation of aggregates and henceforth decreased the DL. The results of EE and DL are given in Table 1.

3.3. Evaluation of optimized NS

3.3.1. FTIR studies

FTIR spectra(s) of pure drug BTF, blank NS and optimized nanosponge (BNS3) were showed in Fig. 3. BTF spectrum showed identical peaks at (3150–3050 cm^{-1}) amine stretching, (2700–2800 cm^{-1}) alkyl stretching, alkyl bending (1600–1900 cm^{-1}) and (550–950 cm^{-1}) alkene bending. Functional group peaks of BTF also have a fingerprint region spectrum. The identical peaks of drug at 3000 cm^{-1}, 2500 cm^{-1}, 1500 cm^{-1} and 800 cm^{-1} were disappeared and shift(s) in the BNS3 NS, these alteration and shifts indicates electrostatic interaction of the drug with the polymers. Furthermore, the fingerprint region analysis of drug molecule in BNS3 NS showed broadening and disappearance of the functional peaks that could be due to drug encapsulation.

3.3.2. DSC studies

DSC Thermograms of pure BTF and BNS3 were presented in Fig. 4. The endothermic DSC curve of a BTF was reflected at 219.41 °C, corresponding to its melting temperature of BTF. DSC curves of BNS3 exhibits a broad endothermic peak, formed by coalescence of EC and BTF as a result of successful drug encapsulation in porous cavities of NS. The disappearance of sharp drug peak and upward line higher than the baseline (exothermic) curve represents fusion of drug with homogenous drug distribution in the polymer, signifies stable BTF loaded NS (Al-Suwayeh et al., 2014).

3.3.3. Scanning electron microscopy

Scanning electron microscopy (SEM) image of the optimized BNS3 as shown in Fig. 5, depicted the spherical, porous and nano-size range of BNS3. The SEM image revealed the porous, spongy feature of NS and it could be due to the in-ward diffusion of DCM in the EC polymeric surface of NS during the fabrication (Al-Suwayeh et al., 2014). The image showed the surface porousness, which could be interrelated with the results of porous material prepared by Chadwick *et.al* (Chadwick et al., 2012).

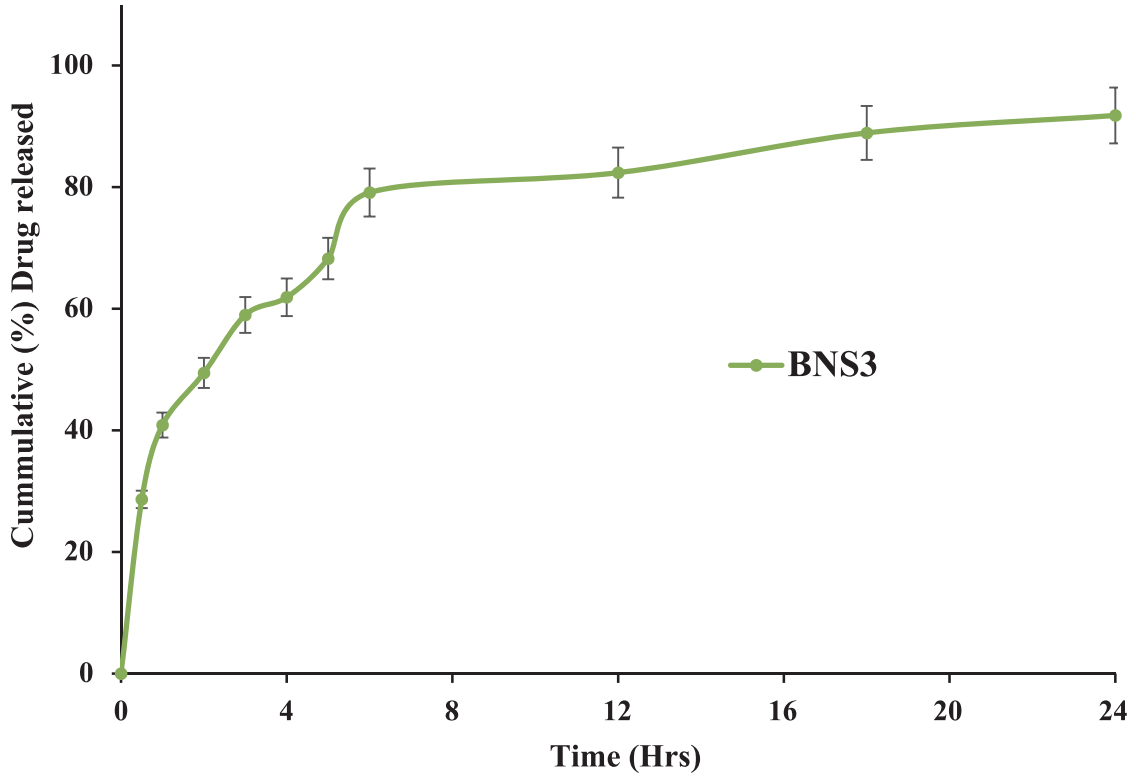

Fig. 6. *In-vitro* drug release of fabricated BNS3 nanosponges.

3.4. Evaluation of topical gel impregnated with BNS3 nanosponge

3.4.1. pH, viscosity, spreadability and drug content estimation

The optimized BTF loaded NS based topical gel showed a pH 6.04 ± 0.30, meet the benchmark pH for skin application. The consistency and spreadability were found to be 36,741 ± 0.76 cps and 14.67 ± 0.76 g-cm/sec, respectively. Drug content estimation BTF was found to be 99.87 ± 0.65%. Viscosity reading was within the topical application range of 35,000–40,000 cps, the rheology study revealed the shear thinning nature (pseudoplastic flow) of the developed topical-gel. As per spreadability value, BNS3 based gel could be easily smear over the applied affected skin area and drug content results showed BTF was homogenously mixed in the nanosponge based gel.

3.4.2. Determination of partition partition, permeation coefficient and flux of drug

The partition coefficient of optimized BNS3 gel was found to be $K_{o/w}$ 3.25, calculated permeability coefficient was (K_p 4.5) with the flux of 0.18 mg/cm^2/h. Permeability coefficient data alone couldn't be sufficient to predict the efficiency of the topical formulation for skin. Flux was considered to be augmentation of the permeability coefficient and concentration of drug in the vehicle/base of the formulation.

3.5. Drug diffusion and release kinetics

The fabricated BNS3 subjected to *in vitro* drug release showed an initial burst release followed by sustained drug release. The initial burst effects at 0.5 h was resultant to the desorption of drug on the NS surface. The porous matrix formed by EC was conferred for sustained and progressive release of BTF. Slow diffusion of water inside the hydrophobic EC lead to a release of drug for prolong period (24 h), (Fig. 6). The cumulative (%) drug release data of the BNS3 was fixed in four mathematical release kinetics model(s) and regression analysis was executed. The results revealed that release fitted into higuchi diffusion kinetic model based on the coefficient of correlation (R^2 values 0.999). Korsmeyer-Peppas model with a diffusion exponent (n values 0.315) represents anomalous non–Fickian release kinetics.

3.5.1. Comparative release studies of BNS3 gel and marketed butenafine cream

The comparative drug release profiles showed 92.88 ± 0.22% BTF release within 3 h for commercial (1% w/w, cream) whereas, BNS3 gel exhibited 89.9 ± 0.15% drug release sustained for up to 24 h (Fig. 7). Relatively slow, less drug release was evident from the release profiles BNS3 gels. This could be due to viscosity that hinders and controlling the drug release.

3.6. In vitro antifungal studies

In-vitro results of antifungal activity performed against two fungal strains is represented in Fig. 8. Zone of inhibition (mm) exhibited for pure BTF (*C. albican*: 10.2 ± 0.2; *A. niger*: 14.3 ± 0.1), BNS3 gel (*C. albican*: 25.5 ± 0.8; *A. niger*: 28.4 ± 0.3) and for commercial fungicidal cream (Product Name with Copyright or TM symbol) (*C. albican*: 15.5 ± 1.2; *A.niger*: 18.7 ± 0.2). It was also established that BTF had more fungicidal activity against *A. niger* as compared to *C. albican* pathogenic fungi. The order of fungicidal activity was found to be BNS3 gel > marketed cream > BTF. According to classification of antimicrobial activity three levels were reported: strong activity if diameter of inhibitory zone (ZI > 20 mm), moderate activity (12 mm < ZI < 20 mm), and weak activity (ZI < 12 mm; As per

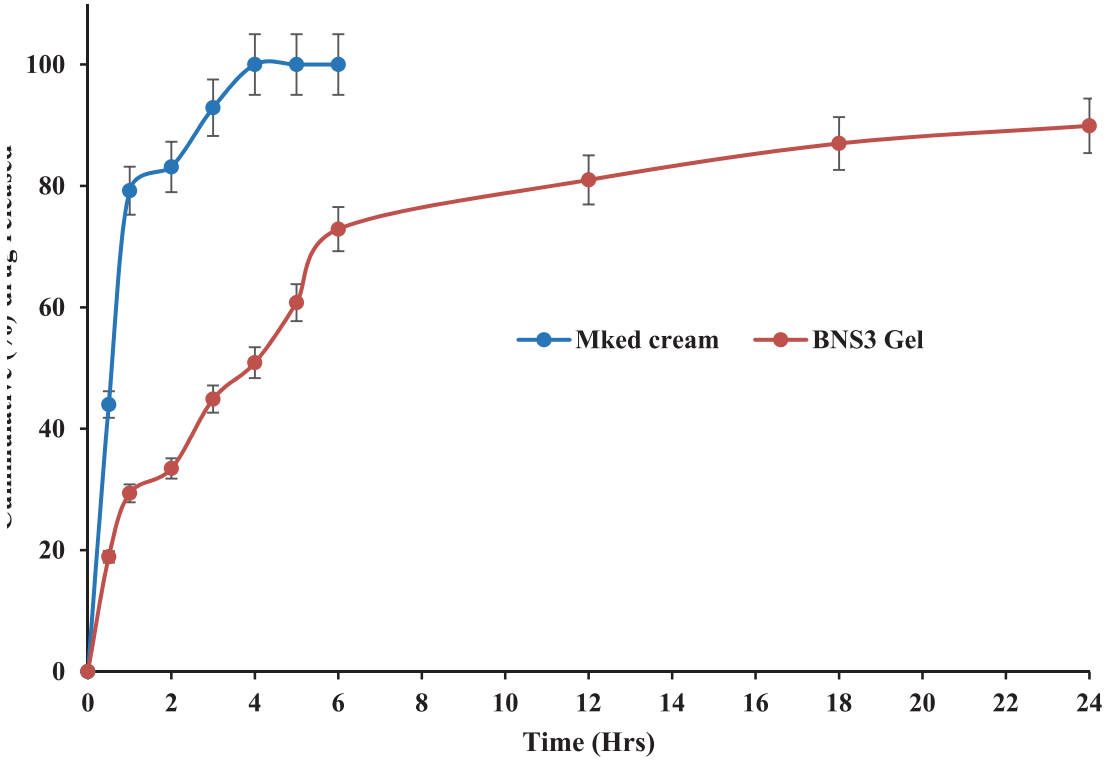

Fig. 7. *In-vitro* drug release of fabricated BNS formulations.

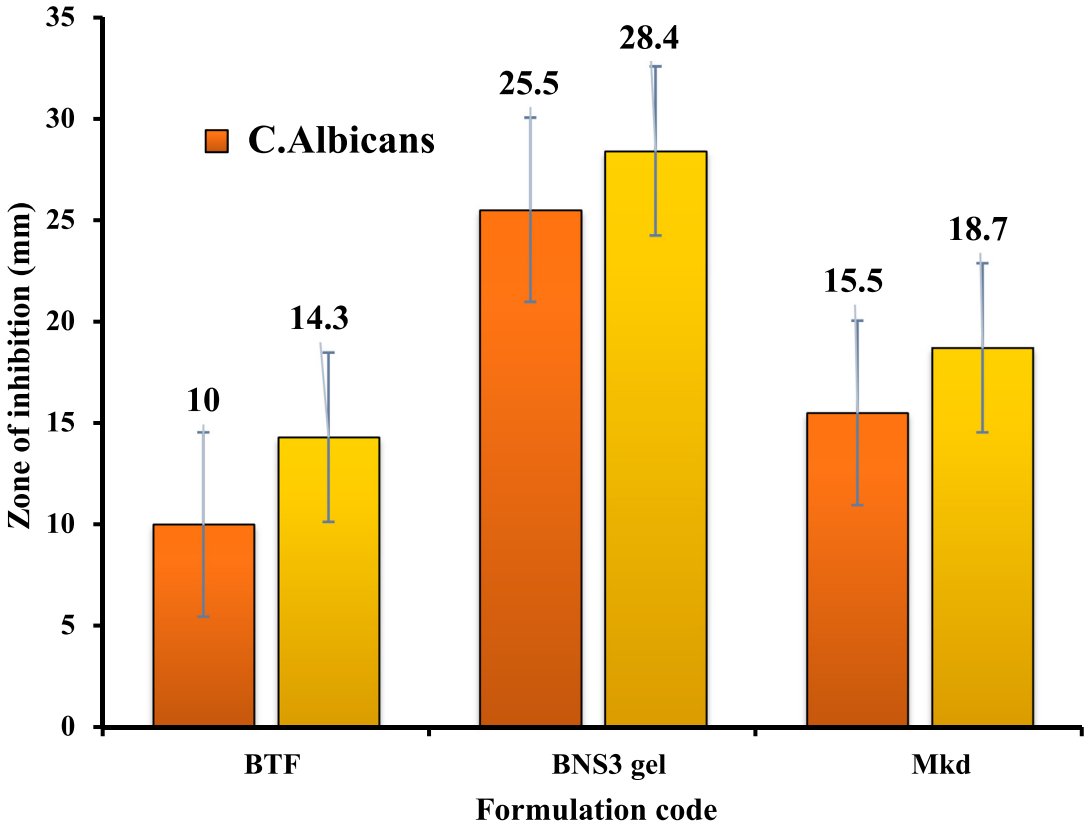

Fig. 8. *In-vitro* antifungal activity of BTF, BNS3 gel and Mked cream.

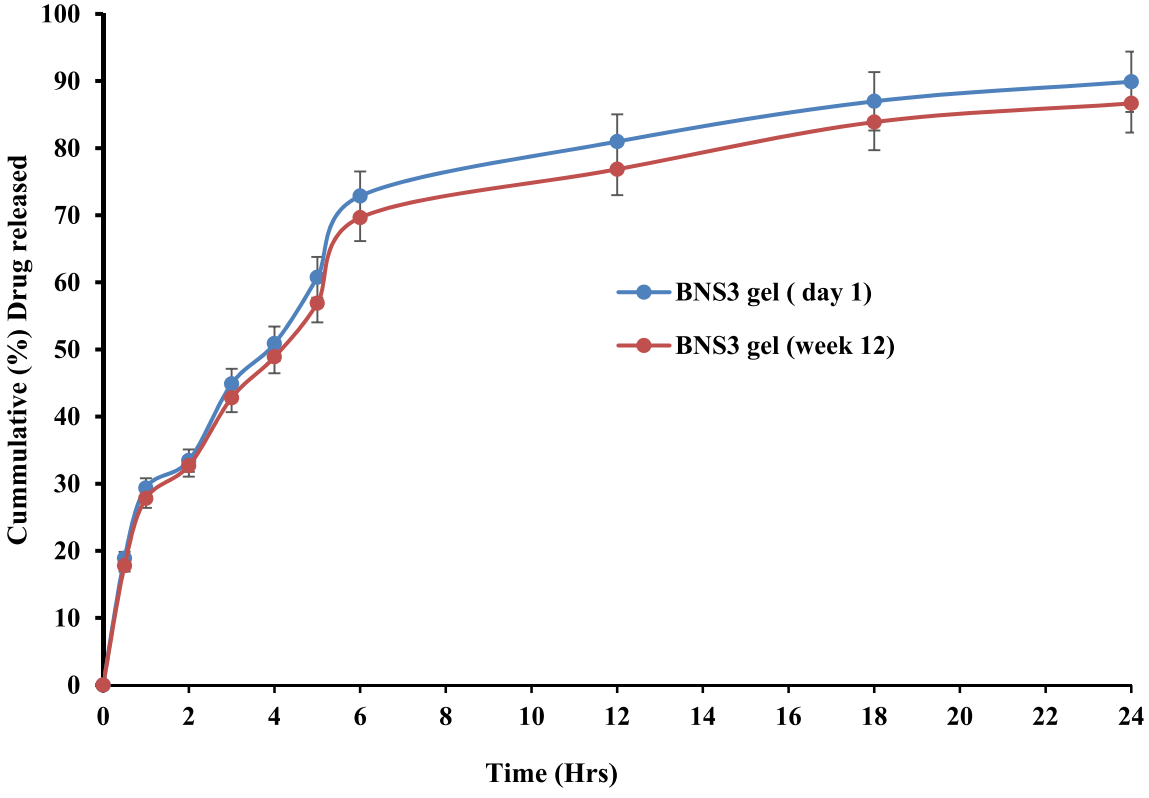

Fig. 9. Stability testing's drug release profiles (day 1 vs week 12).

the clause of antimicrobial activity, distance for ZI classified in highest activity (ZI > 20 mm), moderate (10 mm < ZI < 20 mm) and lowest activity if (ZI < 10 mm). Based on the aforementioned statement the developed BNS3 gel formulation was considered to elucidate the highest fungicidal activity against the selected pathogenic fungal strains.

3.7. Stability studies

The particle size was found to be (543 ± 0.67 nm) and (568 ± 0. 37 nm) for before and after stability testing of BNS3 gel formulation respectively. The variation could be due to storage and imbibing of NS with gel, particle still remain in the nanorange scale. Based on the cumulative % drug release the similarity factor value of BNS3 gel, for before and after stability testing was found to be (f_2: 75) Fig. 9. If the calculated $f2$ ranged between 50 and 100, then drug release profiles considered to be similar and compendia comply. On the ground of particle size and similarity factor ($f2$) BNS3 gel was considered to be stable.

4. Conclusion

The nano based gel formulation is ideal for the effective treatment of fungal infections, since the nanocarrier could permeate the drug deeper into skin layer where other topical semisolid preparations may not reach. Nanocarriers improve therapeutic efficacy by channelizing drug into target site deeper into skin layers for complete eradicated of fungal infections. The developed BTF loaded NS impregnated carbopol polymeric gel could be efficient drug delivery system (DDS) of antifungal agent for the effective treatment of fungal infections by sustaining the drug release, thereby reducing the dosing frequency and reoccurrence of SFI.

Reoccurrence of fungal infection is very often in Candidiasis and Aspergillosis, therefore BNS3 topical gel could be considered as a potential DDS in the treatment of skin-related fungal infections.

Declaration of Competing Interest

The authors declare that they have no known competing financial interests or personal relationships that could have appeared to influence the work reported in this paper.

Acknowledgement

This publication was supported by the Deanship of Scientific Research (DSR) at Prince Sattam Bin Abdulaziz University (PSAU), Al-Kharj, Saudi Arabia.

References

Vyas, A., Kumar Sonker, A., Gidwani, B., 2014. Carrier-Based Drug Delivery System for Treatment of Acne. Sci. World J. 2014, 1–14.

Ahmed, M.M., Anwer, M.K., Fatima, F., Iqbal, M., Ezzeldin, E., Alalaiwe, A., Aldawsari, M.F., 2020a. Development of ethylcellulose based nanosponges of apremilast: In vitro and in vivo pharmacokinetic evaluation. Lat. Am. J. Pharm. 39, 1292–1299.

Ahmed, Mohammad Muqtader, Fatima, F., Mohammed, A.B., 2020b. Olive Oil Based Organogels for Effective Topical Delivery of Fluconazole : In-vitro Antifungal Study 32, 29–36. https://doi.org/10.9734/JPRI/2020/v32i2530821.

Al-Suwayeh, S.A., Taha, E.I., Al-Qahtani, F.M., Ahmed, M.O., Badran, M.M., 2014. Evaluation of Skin Permeation and Analgesic Activity Effects of Carbopol Lornoxicam Topical Gels Containing Penetration Enhancer. Sci. World J. 2014, 1–9.

Anwer, M.K., Al-Mansoor, M.A., Jamil, S., Al-Shdefat, R., Ansari, M.N., Shakeel, F., 2016. Development and evaluation of PLGA polymer based nanoparticles of quercetin. Int. J. Biol. Macromol. 92, 213–219.

Anwer, M.K., Mohammad, M., Ezzeldin, E., Fatima, F., Alalaiwe, A., Iqbal, M., 2019. Preparation of sustained release apremilast-loaded PLGAlga nanoparticles: In vitro characterization and in vivo pharmacokinetic study in rats. Int. J. Nanomed. 14, 1587–1595. https://doi.org/10.2147/IJN.S195048.

Appleton, S.L., Tannous, M., Argenziano, M., Muntoni, E., Rosa, A.C., Rossi, D., Caldera, F., Scomparin, A., Trotta, F., Cavalli, R., 2020. Nanosponges as protein delivery systems: Insulin, a case study. Int. J. Pharm. 590, 119888. https://doi.org/10.1016/j.ijpharm.2020.119888.

Arika, T., Yokoo, M., Hase, T., Maeda, T., Amemiya, K., Yamaguchi, H., 1990. Effects of butenafine hydrochloride, a new benzylamine derivative, on experimental dermatophytosis in guinea pigs.. Antimicrob. Agents Chemother. 34 (11), 2250–2253.

Bautista-Baños, S., Ventura-Aguilar, R.I., Correa-Pacheco, Z., Corona-Rangel, M.L., 2017. Quitosano: Un polisacárido antimicrobiano versátil para frutas y hortalizas en poscosecha -una revisión. Revista Chapingo, Serie Horticultura 23, 103–121. https://doi.org/10.5154/r.rchsh.2016.11.030.

Bergfelt, D.R., 2009. Anatomy and Physiology of the Mare. Equine Breeding Manage. Artif. Insemination 113–131. https://doi.org/10.1016/B978-1-4160-5234-0.00011-8.

Bhosale, S.D., Rajput, S.J., 2011. RP-HPLC method for simultaneous determination of butenafine hydrochloride and betamethasone dipropionate in a cream formulation. Journal of AOAC International 94, 106–109. https://doi.org/10.1093/jaoac/94.1.106.

Bianco, A., Kostarelos, K., Prato, M., 2005. Applications of carbon nanotubes in drug delivery. Curr. Opin. Chem. Biol. 9 (6), 674–679.

Bongomin, F., Gago, S., Oladele, R.O., Denning, D.W., 2017. Global and multi-national prevalence of fungal diseases—estimate precision. J. Fungi 3. https://doi.org/10.3390/jof3040057.

Chadwick, E.G., Beloshapkin, S., Tanner, D.A., 2012. Microstructural characterisation of metallurgical grade porous silicon nanosponge particles. J. Mater. Sci. 47, 2396–2404. https://doi.org/10.1007/s10853-011-6060-0.

Chang, R.K., Raw, A., Lionberger, R., Yu, L., 2013. Generic development of topical dermatologic products: Formulation development, process development, and testing of topical dermatologic products. AAPS J. 15, 41–52. https://doi.org/10.1208/s12248-012-9411-0.

Conte, C., Caldera, F., Catanzano, O., D'Angelo, I., Ungaro, F., Miro, A., Pellosi, D. S., Trotta, F., & Quaglia, F. β-cyclodextrin nanosponges as multifunctional ingredient in water-containing semisolid formulations for skin delivery. J. Pharm. Sci. 103, 2014, 3941–3949. https://doi.org/10.1002/jps.24203.

Danaei, M., Dehghankhold, M., Ataei, S., Hasanzadeh Davarani, F., Javanmard, R., Dokhani, A., Khorasani, S., Mozafari, M.R., 2018. Impact of particle size and polydispersity index on the clinical applications of lipidic nanocarrier systems. Pharmaceutics 10, 1–17. https://doi.org/10.3390/pharmaceutics10020057.

Garg, A., Sharma, G.S., Goyal, A.K., Ghosh, G., Si, S.C., Rath, G., 2020. Recent advances in topical carriers of anti-fungal agents. Heliyon 6, e04663. https://doi.org/10.1016/j.heliyon.2020.e04663.

Gintjee, T.J., Donnelley, M.A., Thompson, G.R., 2020. Aspiring Antifungals: Review of Current Antifungal Pipeline Developments. J. Fungi 6, 28. https://doi.org/10.3390/jof6010028.

Hussain, A., Samad, A., Singh, S.K., Ahsan, M.N., Haque, M.W., Faruk, A., Ahmed, F.J., 2016. Nanoemulsion gel-based topical delivery of an antifungal drug: In vitro activity and in vivo evaluation. Drug Delivery 23, 652–667. https://doi.org/10.3109/10717544.2014.933284.

Kang, E.J., Baek, Y.M., Hahm, E., Lee, S.H., Pham, X.H., Noh, M.S., Kim, D.E., Jun, B.H., 2019. Functionalized β-cyclodextrin immobilized on ag-embedded silica nanoparticles as a drug carrier. Int. J. Mol. Sci. 20. https://doi.org/10.3390/ijms20020315.

Luís, A., Ruela, M., Perissinato, A.G., Esselin, M., Lino, D.S., 2016. Evaluation of skin absorption of drugs from topical and transdermal formulations. Brazilian J. Pharm. Sci. 52, 527–544.

Mahajan, N.M., Zode, G.H., Mahapatra, D.K., Thakre, S., Dumore, N., Gangane, P.S., 2018. Formulation development and evaluation of transdermal patch of piroxicam for treating dysmenorrhoea. J. Appl. Pharm. Sci. 8, 35–41. https://doi.org/10.7324/JAPS.2018.81105.

Manchanda, S., Sahoo, P.K., 2017. Topical delivery of acetazolamide by encapsulating in mucoadhesive nanoparticles. Asian J. Pharm. Sci. 12, 550–557. https://doi.org/10.1016/j.ajps.2017.04.005.

Moglad, H., Fatima, F., Muqtader, M., Devanathad, V., Khalid Anw, M., F. Aldawsa, M., 2020. Development of Topical Antibacterial Gel Loaded with Cefadroxil Solid Lipid Nanoparticles: In vivo Wound Healing Activity and Epithelialization Study. Int. J. Pharmacol. 16, 298–309. https://doi.org/10.3923/ijp.2020.298.309.

Nomura, K., Terwilliger, P., 2019. Biosynthesis, characterization and anti-microbial activity of silver nanoparticle based gel hand wash 577–583.

Omar, S. M., Ibrahim, F., & Ismail, A. 2020. Formulation and evaluation of cyclodextrin-based nanosponges of griseofulvin as pediatric oral liquid dosage form for enhancing bioavailability and masking bitter taste. Saudi Pharm J 28, 349–361. https://doi.org/10.1016/j.jsps.2020.01.016.

Pawar, S., Shende, P., Trotta, F., 2019. Diversity of β-cyclodextrin-based nanosponges for transformation of actives. International J. Pharm. 565, 333–350. https://doi.org/10.1016/j.ijpharm.2019.05.015.

Pudjiastuti, P., Wafiroh, S., Hendradi, E., Darmokoesoemo, H., Harsini, M., Fauzi, M.A. R.D., Nahar, L., Sarker, S.D., 2020. Disintegration, in vitro Dissolution, and Drug Release Kinetics Profiles of k-Carrageenan-based Nutraceutical Hard-shell Capsules Containing Salicylamide. Open Chem. 18, 226–231. https://doi.org/10.1515/chem-2020-0028.

Radaic, A., de Jesus, M.B., Kapila, Y.L., 2020. Bacterial anti-microbial peptides and nano-sized drug delivery systems: The state of the art toward improved bacteriocins. J. Controlled Release 321, 100–118. https://doi.org/10.1016/j.jconrel.2020.02.001.

Rao, M.R.P., Chaudhari, J., Trotta, F., Caldera, F., 2018. Investigation of Cyclodextrin-Based Nanosponges for Solubility and Bioavailability Enhancement of Rilpivirine. AAPS PharmSciTech 19, 2358–2369. https://doi.org/10.1208/s12249-018-1064-6.

Sharma, R., Pathak, K., 2011. Polymeric nanosponges as an alternative carrier for improved retention of econazole nitrate onto the skin through topical hydrogel formulation. Pharm. Dev. Technol. 16, 367–376. https://doi.org/10.3109/10837451003739289.

Shoaib, Q., Abbas, N., Irfan, M., Hussain, A., Arshad, M.S., Hussain, S.Z., Latif, S. Bukhari, N.I. Development and evaluation of scaffold-based nanosponge formulation for controlled drug delivery of naproxen and ibuprofen. Tropical J Pharm Res 17, 2018. doi: 10.4314/tjpr.v17i8.2.

Shukr, M.H., Metwally, G.F., 2013. Evaluation of Topical Gel Bases Formulated with Various Essential Oils for Antibacterial Activity against Methicillin Resistant Staphylococcus Aureus. Tropical. J Pharm Res 12, 877–884.

Sousa, M.G.C., Maximiano, M.R., Costa, R.A., Rezende, T.M.B., Franco, O.L., 2020. Nanofibers as drug-delivery systems for infection control in dentistry. Expert Opinion on Drug Delivery 17, 919–930. https://doi.org/10.1080/17425247.2020.1762564.

Srikar, G., Rani, A.P., 2019. Study on influence of polymer and surfactant on in vitro performance of biodegradable aqueous-core nanocapsules of tenofovirdisoproxil fumarate by response surface methodology. Brazilian J. Pharm. Sci. 55, 1–11. https://doi.org/10.1590/s2175-97902019000118736.

Trotta, F., Zanetti, M., Cavalli, R., 2012. Cyclodextrin-based nanosponges as drug carriers. Beilstein J. Org. Chem. 8, 2091–2099. https://doi.org/10.3762/bjoc.8.235.

Varan, C., Anceschi, A., Sevli, S., Bruni, N., Giraudo, L., Bilgiç, E., Korkusuz, P., İskit, A. B., Trotta, F., & Bilensoy, E. 2020. Preparation and characterization of cyclodextrin nanosponges for organic toxic molecule removal. Int J Pharm 585, 119485. https://doi.org/10.1016/j.ijpharm.2020.119485.

Ventola, C.L., Bharali, D.J., Mousa, S.A., 2010. The Nanomedicine Revolution: Part 1: Emerging Concepts. Pharm. Therap. 128, 512–525.

Yang, X., Trinh, H.M., Agrahari, V., Sheng, Y., Pal, D., Mitra, A.K., 2016. Nanoparticle-Based Topical Ophthalmic Gel Formulation for Sustained Release of Hydrocortisone Butyrate. AAPS PharmSciTech 17, 294–306. https://doi.org/10.1208/s12249-015-0354-5.

Yapar, N., 2014. Epidemiology and risk factors for invasive candidiasis. Ther. Clin. Risk Manag. 10, 95–105. https://doi.org/10.2147/TCRM.S40160.